BRAIN
ORIGINAL ARTICLE

A neural network for tics: insights from causal brain lesions and deep brain stimulation

Christos Ganos,[1,†] Bassam Al-Fatly,[1,†] Jan-Frederik Fischer,[1] Juan-Carlos Baldermann,[2,3] Christina Hennen,[2] Veerle Visser-Vandewalle,[4] Clemens Neudorfer,[1] Davide Martino,[5,6] Jing Li,[7] Tim Bouwens,[8] Linda Ackermanns,[8] Albert F. G. Leentjens,[9] Nadya Pyatigorskaya,[10] Yulia Worbe,[11] Michael D. Fox,[7,12] Andrea A. Kühn[1,†] and Andreas Horn[1,7,†]

[†]These authors contributed equally to this work.

Brain lesions are a rare cause of tic disorders. However, they can provide uniquely causal insights into tic pathophysiology and can also inform on possible neuromodulatory therapeutic targets. Based on a systematic literature review, we identified 22 cases of tics causally attributed to brain lesions and employed 'lesion network mapping' to interrogate whether tic-inducing lesions would be associated with a common network in the average human brain. We probed this using a normative functional connectome acquired in 1000 healthy participants. We then examined the specificity of the identified network by contrasting tic-lesion connectivity maps to those seeding from 717 lesions associated with a wide array of neurological and/or psychiatric symptoms within the Harvard Lesion Repository. Finally, we determined the predictive utility of the tic-inducing lesion network as a therapeutic target for neuromodulation. Specifically, we collected retrospective data of 30 individuals with Tourette disorder, who underwent either thalamic ($n = 15$; centromedian/ventrooralis internus) or pallidal ($n = 15$; anterior segment of globus pallidus internus) deep brain stimulation and calculated whether connectivity between deep brain stimulation sites and the lesion network map could predict clinical improvements.

Despite spatial heterogeneity, tic-inducing lesions mapped to a common network map, which comprised the insular cortices, cingulate gyrus, striatum, globus pallidus internus, thalami and cerebellum. Connectivity to a region within the anterior striatum (putamen) was specific to tic-inducing lesions when compared with control lesions. Connectivity between deep brain stimulation electrodes and the lesion network map was predictive of tic improvement, regardless of the deep brain stimulation target.

Taken together, our results reveal a common brain network involved in tic generation, which shows potential as a therapeutic target for neuromodulation.

1 Charité – Universitätsmedizin Berlin, corporate member of Freie Universität Berlin and Humboldt-Universität zu Berlin, Movement Disorders and Neuromodulation Unit, Department of Neurology with Experimental Neurology, 10117 Berlin, Germany
2 Department of Psychiatry and Psychotherapy, Faculty of Medicine and University Hospital Cologne, University of Cologne, 50931 Cologne, Germany
3 Department of Neurology, Faculty of Medicine and University Hospital Cologne, University of Cologne, 50931 Cologne, Germany
4 Department of Stereotactic and Functional Neurosurgery, Faculty of Medicine and University Hospital Cologne, University of Cologne, 50931 Cologne, Germany
5 Department of Clinical Neurosciences, University of Calgary, Calgary 3330, AB, Canada

Received September 7, 2021. Revised November 14, 2021. Accepted December 16, 2021. Advance access publication January 13, 2022

6 Hotchkiss Brain Institute, Calgary 3330, AB, Canada
7 Center for Brain Circuit Therapeutics, Department of Neurology, Psychiatry, and Radiology, Brigham and Women's Hospital, Harvard Medical School, Boston, MA 02115, USA
8 Department of Neurosurgery, Maastricht University Medical Centre, 6229 HX Maastricht, The Netherlands
9 Department of Psychiatry, Maastricht University Medical Centre, 6229 HX Maastricht, The Netherlands
10 Sorbonne University, Paris Brain Institute - ICM, Inserm, CNRS, Department of Radiology, Hôpital de la Pitié Salpêtrière (DMU 6), AP-HP, 75013, Paris, France
11 Sorbonne University, ICM, Inserm, CNRS, Department of Neurophysiology, Hôpital Saint Antoine (DMU 6), AP-HP, 75013 Paris, France
12 Athinoula A. Martinos Centre for Biomedical Imaging, Department of Neurology and Radiology, Massachusetts General Hospital, Charlestown, MA 02129, USA

Correspondence to: Andreas Horn
Movement Disorders and Neuromodulation Unit
Department of Neurology
Charité University Medicine Berlin
Charitéplatz 1, 10117 Berlin, Germany
E-mail: andreas.horn@charite.de

Keywords: brain lesions; tic disorders; lesion network mapping; deep brain stimulation

Introduction

Tics are brief and sudden movements or sounds that resemble voluntary actions but occur repetitively and without embedment to discernible context.[1] Tics may have multiple aetiologies, but they are most encountered as part of a neurodevelopmental disorder spectrum, including Tourette disorder, which affects ~1% of children. There has been a long-standing debate about the pathophysiological underpinnings of tics and in the past few decades there have been numerous efforts to identify the neuronal locus—or network—that leads to their emergence.[2,3]

The basal ganglia have been suggested as key neuronal structures in tic genesis.[4] This was driven by neuropathological studies, which identified abnormalities within motor and associative functional domains of the striatum and globus pallidus internus (GPi),[5,6] and therapeutic interventions, such as deep brain stimulation (DBS) that targeted these areas. Building on ablational studies by Hassler and Dieckmann,[7] a first report on a patient treated with DBS targeting the border between centromedian and ventrooralis internus nuclei of the thalamus (CM-Voi) was published in 1999.[8] Since then, DBS targeting (i) this target[9,10]; (ii) the anterior versus posterior ventrooralis nuclei in Hassler nomenclature[11] (or ventroanterior/ventrolateral thalamus according to Jones nomenclature[12]); (iii) the anteromedial[13,14]; and (iv) the posteroventral[15] GPi has been demonstrated to effectively reduce tics. More recently low-frequency tic-related neuronal activity was recorded in GPi and CM-Voi in Tourette patients undergoing DBS suggesting an electrophysiological correlate in tic pathophysiology.[16,17,18]

Outside the basal ganglia, cortical neurophysiology studies have implicated the supplementary motor area and primary motor cortex in tic occurrence.[17–19,20,21,22] Structural and functional neuroimaging studies further revealed an extensive network of additional brain areas involved in the generation of tics (reviewed by Martino *et al.*[23]), including the prefrontal and cingulate cortices,[24,25,26] the primary somatosensory area,[24,25–27,28,29,30] the parietal operculum[31,32] and the insula.[27–31,32,33]

These and other studies suggest that tics are not the result of a single dysfunctional brain region, but rather emerge in consequence of critical alterations at different cortical and subcortical hubs within a widespread neural circuit.[24–34] However, a causal role of different brain regions for tic generation remains elusive. Moreover, while some regions described in functional (correlative) studies may contribute to tic expression, others could indeed be involved in symptom compensation.

Studies of brain lesions and brain stimulation results are among the few general concepts that may justify causal inference.[35] More recently, it has become possible to map the impact of specific lesions on distributed 'brain networks'. The technique, termed 'lesion network mapping'[36] uses normative functional connectomes acquired in large samples of healthy participants to investigate into which network a specific lesion would fall in the average human brain. So far, the method has provided insights into different neuropsychiatric symptoms,[35] including movement disorders[37,38,39] and disorders of volition.[40,41] In a similar vein, a novel concept termed 'DBS network mapping' has applied the same concept to stimulation sites.[42] Again, the method asks the question of which functional brain network a specific DBS stimulation site would fall within the average human brain. So far, the method has provided insights into effective neuromodulation networks in neurological disorders of movement[42,43,44] and psychiatric disorders.[45,46] Importantly, several papers have shown that both lesion and DBS network mapping provide convergent results, as for example in parkinsonism,[38] dystonia[39] and depression.[47]

The aim of this study was to shed light onto the networks associated with tic generation using combined brain lesion and DBS network mapping. To this end, we carried out a systematic review of the medical literature to collect brain lesions that were involved in the occurrence of tics and determined the common functional network underlying most lesions. To assess the therapeutic relevance of this network, we predicted clinical outcomes in patients with Tourette disorder who received therapeutic DBS (either in the CM-Voi of thalamus or GPi) from three different centres (Cologne, Paris and Maastricht).

Materials and methods

Cases and lesion definition

Methods of the review were developed by two members of the author team (C.G., J.F.F.) prior to conducting the review. In March 2020

PubMed (MEDLINE 1966–2020) and EMBASE (1947–2020) were searched with a combination of free-text, MeSH terms, and truncated words (Supplementary material). To be included, papers needed to meet predefined inclusion criteria: (i) English reports; describing (ii) patients (case reports, case series, letters and observational studies); with (iii) new-onset tics; attributed to (iv) lesions of the CNS; and (v) lesion location shown by neuroimaging that was further described in writing. After removal of duplicates results were screened by title and abstract. The first 50 abstracts were screened by two reviewers (J.F.F., C.G.) to control for interpersonal agreement and subsequent results were screened by one author (J.F.F.). Eligible, and available records were then read in full text subsequently. If the single reviewer had questions about the potential full-text inclusion of an article, the full text was then reviewed with the first author (C.G.) for discussion. Risk of bias assessment was not applicable. Details on the number of results and the process of literature search are listed in Supplementary Fig. 1. We did not apply a temporal restriction criterion between the clinical manifestation of tics and the documentation of brain lesions to capture as many different aetiologies as possible. In cases where the manifestation of tics was the only clinical event associated with a brain lesion, we captured the latency between the two. In all other cases, where an additional clinical syndrome preceded the onset of tics and was attributed to documented brain damage, we captured the time lag between this event, tic behaviours and lesion confirmation. We excluded reports about 'tic-like' phenomena, which may subsume functional tic disorders or overlap syndromes, as well as drug-induced tics and cases of tics associated with traumatic events of the peripheral nervous system. Reports of tic improvement associated with brain lesions (e.g. through neurosurgery) were not considered. Cases with characteristic brain malformations associated with known, mostly neurodevelopmental, genetic syndromes and tic disorders were also excluded. Review articles were included for cross-referencing in the first step.

From the included reports we extracted the following data: (i) study characteristics (study type, year of publication); (ii) patient characteristics (age of assessment, sex, medical history, type of clinical event and age at time of occurrence); (iii) clinical characteristics of tics (predisposing factors, pre-existing tics and their characteristics, latency between first confirmation of lesions and tic onset/worsening, motor/vocal forms, tic somatotopy, suppressibility/premonitory urges, waxing and waning course, neuropsychiatric comorbidities, therapeutic strategy and outcome and additional video documentation); and (iv) characteristics of documented brain lesion (attributed aetiology, anatomical localization and modality of neuroimaging, age at confirmation of lesion).

Lesion locations were identified from corresponding publication figures and manually traced using 3D Slicer (www.slicer.org) on a common T_1 template available within ICBM2009b NLIN Asym ('MNI') space.

Lesion network mapping

Each binary lesion mask was entered as a seed using the Lead connectome mapper toolbox openly available within Lead-DBS (www.lead-dbs.org[48]). Seed-based connectivity was calculated using a normative functional MRI connectome acquired at rest in 1000 participants[49] that had been preprocessed as described elsewhere.[50] For each subject in the connectome, blood oxygen level-dependent (BOLD) signal fluctuations across all voxels within the lesion mask were averaged and correlated to the BOLD signal of all other brain voxels using the Pearson correlation coefficient. This resulted in 1000 *R*-values for each brain voxel (one per subject) which were Fisher z-transformed. Using voxel-wise one-sample T-tests, these 1000 *z*-values were summed up to an average connectivity profile map of T-scores. We will refer to this map as the T-map. Every lesion specific T-map was then thresholded to a T-score of 7 and binarized to represent the significant positive T-scores in each T-map. This threshold level was chosen based on previous experience in multiple lesion network mapping publications (see Cohen and Fox[51] for a discussion). Choosing a range of different thresholds largely did not alter the overall pattern of the result (Supplementary Fig. 2). In a next step, all lesion-specific binarized T-maps ($n = 22$) were summed up into a single N-map which represented a tic-inducing lesion network map (LNM). The LNM was then thresholded to include only voxels that received contribution from ≥19/22 lesions (86% of cases). This threshold was chosen upon visual inspection and the number of retained voxels, to define a set of regions most specifically connected to a maximum number of lesion cases (higher thresholds >20 or >21 retained little to no voxels, see Supplementary Fig. 3 for results with different thresholds).

Specificity of tic lesion network

We then aimed to explore whether specific sites within the tic-lesion network were not only sensitive but also specific to tics compared to other naturally occurring brain lesions. In order to do so, connectivity T-maps derived from tic-inducing lesions were compared to the ones from a total of 717 other brain lesions from the Harvard Lesion Repository.[35] This repository contains lesions associated with various neurological and/or psychiatric symptoms which are (numbers indicate lesion counts in each specific category): Akinetic Mutism, 28; Alien Limb, 53; Amnesia, 53; Aphasia, 12; Asterixis, 30; Cervical Dystonia, 25; Criminality, 17; Delusions, 32; Depression, 58; Freezing of gait, 14; Hemichorea 29, Hallucination: 89, Holmes' tremor, 36; Infantile Spasms, 74; Loss of consciousness, 16; Mania, 56; Pain, 22; Parkinsonism, 29; Prosopagnosia, 44. The specificity map was calculated using a voxel-wise permutation-based two-sample T-test performed (with 1000 permutations) within FSL PALM (https://fsl.fmrib.ox.ac.uk/fsl/fslwiki/Randomise/UserGuide). A rigorous voxel-wise family-wise error (FWE) correction was then applied at $\alpha < 0.05$ to reduce false positive results[52] and highlight only the significant findings. Based on these results, we subsequently computed a 'conjunction map', on which voxels that were both specific and sensitive to tics were retained by multiplying the sensitivity (lesion network) map and the specificity map.

Relationship to DBS treatment

In a further step, we sought to investigate the relevance and potential clinical utility of the tic-inducing lesion network. We tested whether specific stimulation sites in a retrospective cohort of Tourette disorder patients treated with DBS that were maximally connected to the lesion network map would be associated with optimal outcomes. Pre- and postoperative imaging data from a total of 30 adult patients from three DBS centres with a diagnosis of Tourette disorder that underwent DBS surgery were used to localize DBS electrodes and specify stimulation sites in each patient.

Fifteen adult patients with Tourette disorder underwent DBS to thalamus nuclei (Cologne cohort; $n = 12$ in the centromedian-ventro-oralis and $n = 3$ in the nucleus ventroanterior/ventrolateral nucleus with the most distal contacts residing in the field of Forel/subthalamic nucleus) and 15 to the GPi (Paris and

Maastricht cohorts). Localization of electrodes and estimation of stimulation volumes were carried out using Lead-DBS software (www.lead-dbs.org[48]). We applied default parameters of the revised pipeline.[53] Briefly, this involved co-registration between post-operative MRI ($n = 2$) or CT ($n = 28$ patients) to preoperative anatomical MRIs using advanced normalization tools (ANTs; http://stnava.github.io/ANTs/[54]). The resulting co-registered images were then normalized to MNI space using the ANTs SyN Symmetric Diffeomorphic algorithm[54] using the 'effective: low variance + subcortical refinement' preset in Lead-DBS. Electrodes were reconstructed using the PaCER[55] algorithm and manually refined, if necessary. Stimulation volumes were estimated using a finite element approach based on a four-compartment tetrahedral mesh (including white or grey matter, electrode insulating and conducting regions).[53] The estimated E-field was thresholded to a heuristic value of 0.2 V/mm to calculate the extent of a binary volume. These were then used as seed regions to calculate functional connectivity average T-scores, representing average connectivity strength, to voxels within the tic-inducing lesion network. T-scores were z-transformed to a Gaussian distribution following the approach of van Albada *et al.*[56] to serve as predictors of DBS associated tic-improvements.

In a last step, we sought to investigate how connectivity strength from stimulation sites of DBS cohorts to both sensitive and specific voxels of the maps, and their overlap (conjunction map) could explain tic-improvement. Similar to the analysis above, connectivity strength was again calculated between DBS stimulation sites and the respective map. These coefficients were then correlated to tic-improvement.

DBS network mapping

In a final analysis, we aimed at characterizing the networks optimally modulated by each DBS site in a data-driven fashion. To do so, we applied DBS network mapping following the approach by Horn *et al.*,[42] which follows a highly similar logic as the lesion network mapping approach. Briefly, DBS network maps were calculated in identical fashion to lesion network maps. We then correlated connectivity strength in each voxel with tic improvements, across patients, resulting in R-map models that approximate optimal connectivity profiles. Voxels with high values on these maps embody locations to which DBS electrodes that led to optimal improvement were strongly connected. We calculated these R-map models for each target cohort separately (pallidal and thalamic target). In a second step, we multiplied resulting maps with each other, but only retaining voxels that were positive on both maps. In doing so, we were able to pinpoint the network from two angles (pallidal and thalamic DBS sites). Therefore, this approach would likely clean the result from some spurious correlations and retain a higher fraction of regions that could indeed have causal implications.[57]

Data availability

The DBS MRI/CT datasets generated and analysed during the current study are not publicly available due to data privacy regulations of patient data but are available from the corresponding author upon reasonable request. Lesion network map and code used to analyse the datasets is available within Lead-DBS/-Connectome software (https://github.com/leaddbs/leaddbs).

Results

The systematic review (see Supplementary Fig. 1 for flow chart) identified 22 cases with new onset of tics attributed to brain lesions (Supplementary Table 1). The mean age at tic onset was 25.3 years [±20.7 standard deviation (SD), range 5–73 y; in two cases tic-onset age was not provided]. In 12 cases, the latency between brain injury and tic onset could be reconstructed (Supplementary Table 1). There were two cases with isolated motor tics and two with isolated vocal tics. The remaining 18 cases had both motor and vocal tics. Premonitory urges and tic suppressibility were documented in 10 and 12 cases, respectively. In 10 cases, additional movement disorders were also noted, including dystonia ($n = 4$), parkinsonism ($n = 3$), cerebellar ataxia ($n = 2$), tremor ($n = 1$) and stereotypies ($n = 1$). However, again, in these cases occurrence of tics was salient and novel following the brain lesion. Neuropsychiatric features, such as impulsivity and/or hyperactivity ($n = 9$), obsessive-compulsive ($n = 5$) and self-injurious behaviours ($n = 3$) were also reported.

Although the basal ganglia were the most commonly documented lesion site ($n = 17$), the locus of neuronal damage varied among cases, and often involved multiple brain areas (Fig. 1). Other brain areas included the temporal and parietal lobes, the insula, corpus callosum, thalamus, internal capsule, midbrain, pons and medulla oblongata. Brain lesions occurred for different aetiological reasons, ranging from traumatic brain injury to stroke, as well as infectious and inflammatory causes (Supplementary Table 1 provides the complete list of clinical and paraclinical case characteristics).

Although tic-inducing brain lesions expressed spatial heterogeneity, they mapped to a common functional brain network (Figs 2 and 3). Namely, voxels within a network comprising the insular cortices, cingulate gyrus, striatum, GPi, thalami, and the cerebellum were connected to a majority of lesions (Fig. 3 and Table 1). This included thalamic and pallidal DBS targets (Fig. 3 insets).

However, while the identified network seemed sensitive to tic-inducing lesions, it did not provide insights into how specific it would be to tics. In other words, while spontaneously occurring lesions associated with tics formed part of the network, this did not preclude lesions associated with different symptoms would not fall into the network, as likely. To account for this, we probed the specificity of the identified network by contrasting tic lesion connectivity maps with connectivity maps seeding from 717 lesions within the Harvard Lesion Repository that were associated with a wider array of neurological and/or psychiatric symptoms. This showed significantly higher connectivity of tic-inducing (versus control) lesions to the anterior striatum (Fig. 4B). Subsequent conjunction analysis identified voxels that were both sensitive and specific to tics (Fig. 4C).

To probe the predictive utility and therapeutic significance of the identified tic-inducing network, we calculated connectivity between DBS stimulation sites in 30 patients with Tourette disorder (Fig. 5) and the lesion network. Connectivity strength correlated with respective tic improvements in both pallidal and thalamic cohorts when analysed together ($R = 0.45$ at $P = 0.01$) and each DBS target separately (thalamic target: $R = 0.54$ at $P = 0.01$; GPi target: $R = 0.45$ at $P = 0.04$; Fig. 6). Connectivity between DBS stimulation sites and the specific and conjunction maps also correlated with clinical improvements ($R = 0.43$ at $P = 0.004$, $R = 0.43$ at $P = 0.006$; Fig. 6B).

In a final analysis, we wanted to probe optimal DBS connectivity profiles in a data-driven fashion. We did so by correlating connectivity values with clinical improvements for each cohort, in a voxel-wise fashion (following the approach of Horn *et al.*[42]). This resulted in a set of connections with differences and similarities for the

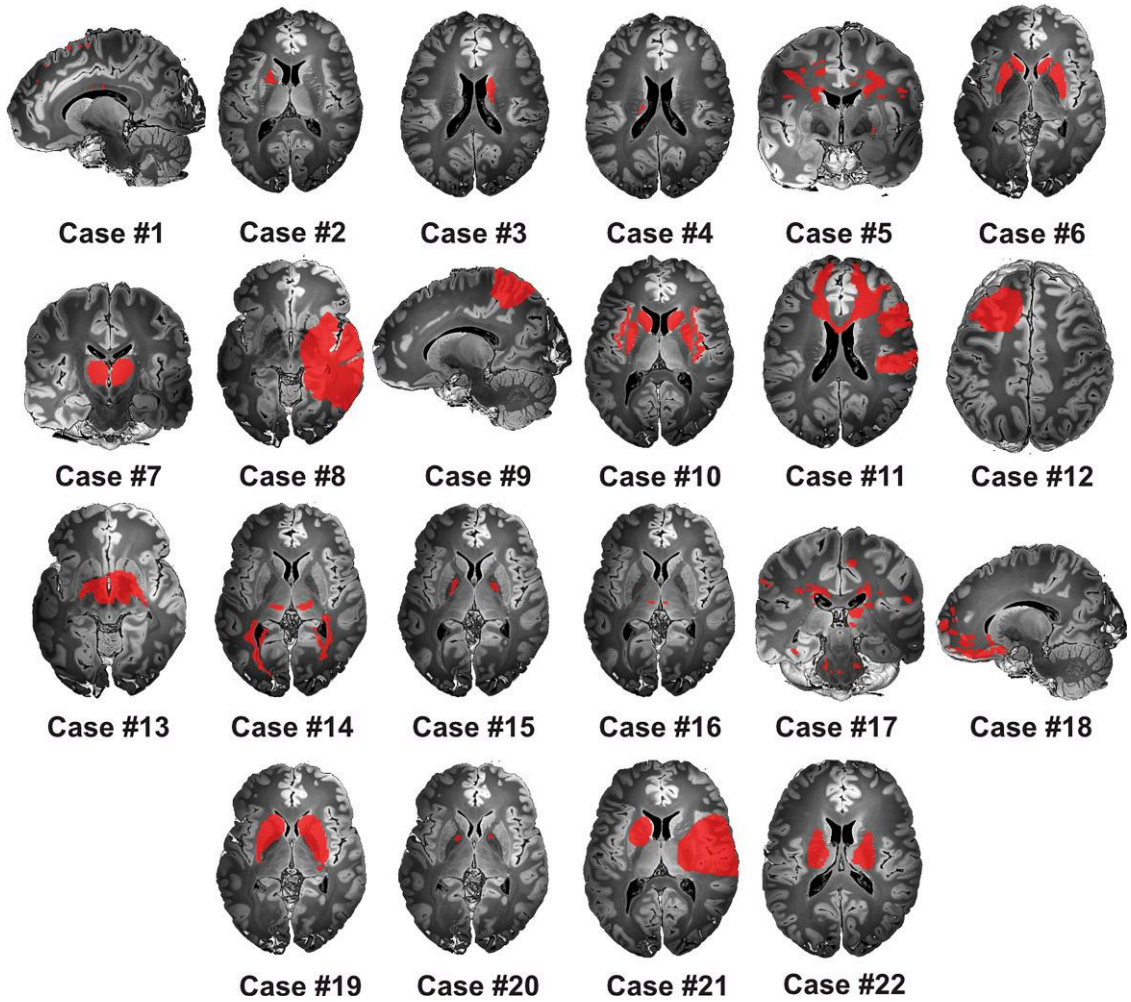

Figure 1 Tic-inducing lesions. The spatial distribution of lesion masks extracted from 22 case reports included in the current study mapped to a wide extent of brain regions. All binary masks were drawn in MNI space and visualized on an ultra-high resolution post-mortem template for anatomical reference.[58]

pallidal and thalamic DBS sites. While some sites of optimal connectivity agreed between DBS sites, the two maps were largely different (Fig. 7). However, when probing which regions had positive associations with clinical outcomes for both sites (thalamic and pallidal DBS), this carved out a network that included a highly similar pattern of regions as did the lesion network (Fig. 7 and Table 1). Hence, by pinpointing the sites of optimal connectivity for effective DBS from two DBS targets, a more specific network emerged that matched the one defined by tic-inducing brain lesions.

Discussion

Three major conclusions can be drawn from this study. First, our results confirm that a network of brain regions is involved in tic generation. Second, we show that a sub-region of the anterior striatum shows specificity to tics when comparing lesion network results to a larger database of lesions associated with other neurological and/or psychiatric symptoms. Third, the identified network was able to predict outcomes following DBS in cohorts with two subcortical stimulation targets.

A tic-inducing neural network

Contemporary neurology and neuropsychiatry in part explain pathological changes of behaviour as a result of damage to distributed brain networks rather than to isolated brain regions.[35] In this sense, behavioural brain network disorders have been described as 'circuitopathies' or 'connectopathies'.[59,60] In the rare cases of lesion-induced tics identified by our systematic search, the inciting lesions were connected to a common neural circuit, which encompassed structures of the cortico-basal-ganglia-thalamo-cortical circuit, as well as the insular and anterior cingulate cortex (ACC). These regions have previously been implicated in the pathophysiology of tic disorders.[23] For example, in their seminal functional MRI study on the neural correlates of tics, Bohlhalter *et al.*[31] identified a network that preceded tic onset which largely overlapped with the present network, including the insular cortex, ACC, putamen, and thalamus. The relevance of these structures was confirmed in a subsequent study, which employed a similar design with careful time-locked monitoring of tics, providing further support to their involvement in tic occurrence.[32] Moreover, the insular cortex and the ACC have also been associated with specific pathophysiologic aspects of tic occurrence, including premonitory urges[33] and vocalizations.[61] Of note, the role of the input and output

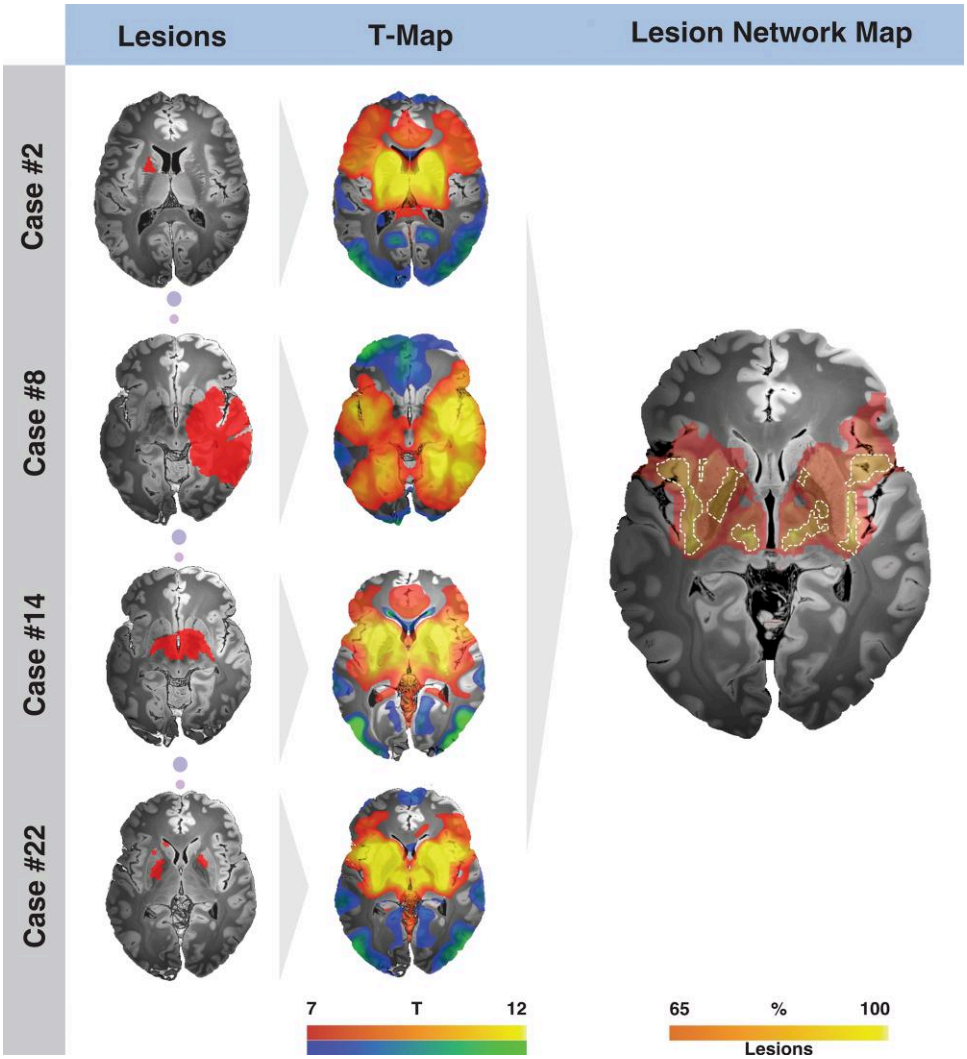

Figure 2 Exemplary cases illustrating the methodological steps used to create the lesion network map. Each lesion mask (*left*) extracted from the literature ($n = 22$) served as a seed region using normative rs-fMRI connectivity data acquired in 1000 healthy participants. The resulting connectivity profiles (in form of T-maps aggregated across the 1000 rs-fMRI scans) were then thresholded and summed to identify regions connected to most tic-inducing lesions (*right*). The final lesion network map features brain regions connected to voxels encompassed by at least 19 of the 22 identified patient-specific lesion maps.

structures of the basal ganglia in tic emergence had already been highlighted by pioneering neuropathological studies in the field[5,6–62] and Hassler's and Dieckman's early neurosurgical therapeutic interventions for tics and obsessive-compulsive symptoms.[7] Indeed, the thalamic and GPi clusters of the network we have identified precisely matched the ablational lesion locations probed by these pioneering studies and showed overlap with the common DBS targets used for the treatment of Tourette disorder (which were inspired by them).[63]

Finally, the network associated with tics identified here covers the claustrum, which could be of potential interest. While the function of the claustrum remains somewhat elusive (and it has been seen as an additional cortical layer by some authors, e.g. Swanson[64]), lesion network mapping has associated a specific part of the claustrum with the occurrence of lesion-induced parkinsonism.[38] Similar to all parts of the basal ganglia, the claustrum is a widespread structure with inputs and outputs from and to various cortical regions, including connecting the anterior insula with the ACC.[65] Hence, specific parts of the structure could be involved in motor processing (and potentially the occurrence of tics), while others would be involved in cognitive or limbic processes.

A specific role for the anterior striatum in tic induction

The comparison between individual tic lesion network profiles and a large database of cases with lesions associated with neurological and psychiatric disorders revealed a specific role of the anterior striatum in tic induction, which was identified as a subset of the tic-related lesion network. Conjunction analysis identified a region within the anterior putamen, which was both sensitive and specific to tics. This region mapped to the associative-limbic functional zone of the striatum,[66] well within the projection site of CM-Voi. Importantly, this pre-commissural sub-region of the putamen constitutes a complex information processing hub, driven by its exceptional level of input heterogeneity.[67] Similarly, CM-Voi nuclei receive input from and diffusely project to the entire cerebral cortex.[68] A compelling pathological study of brains of adults with

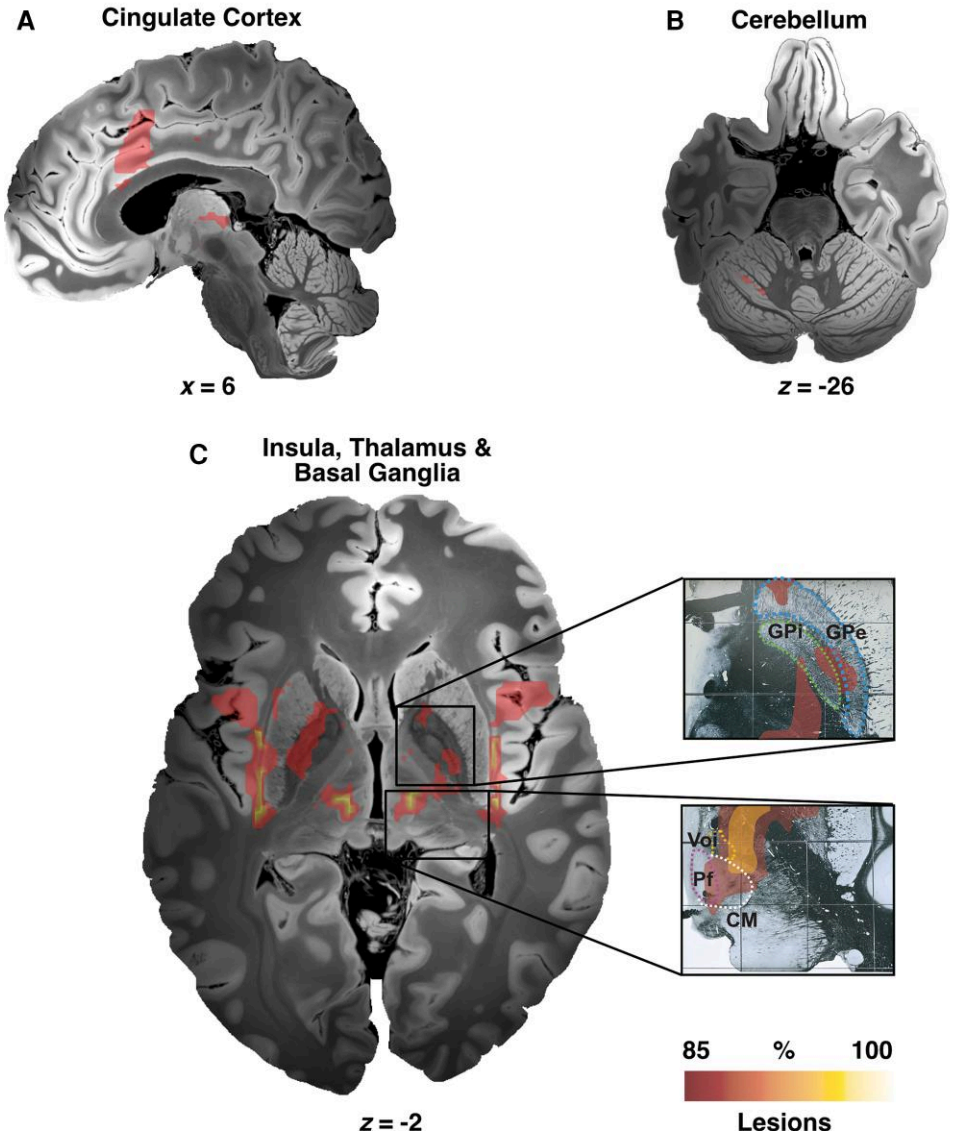

Figure 3 Tic-inducing lesion network map. Lesion network mapping highlighted different cortical and subcortical regions including cingulate cortex (**A**), cerebellum (lobule VI) (**B**), insula, thalamus, striatum, and the pallidum (**C**). Of note, main DBS neuroanatomical targets (GPi and CM-Pf-Voi) used to treat primary tic-syndrome are included within the network. CM = centromedian nucleus of thalamus; GPe = globus pallidus externus; GPi = globus pallidus internus; Pf = parafascicular nucleus of thalamus; Voi = ventralis oralis nucleus of thalamus.

Tourette disorder reported pronounced decreases of different interneuronal populations in the associative and, to a lesser degree, sensorimotor striatum.[6] At the same time, animal models of pharmacologically-induced GABAergic disinhibition within this sub-region of the striatum led to tic-like behaviors.[69,70] This body of pathological and behavioural animal model data suggests that information processing within this striatal hub, and its functional connectivity with other subcortical structures, could be altered in primary tic disorders.

A tic-lesion network as a potential target for neuromodulation

Tic disorders are characterized by clinical heterogeneity and variability in treatment response, including response to DBS.[63] According to a recent estimate, ~30% of adults with Tourette disorder and moderate to severe tics are refractory to non-invasive interventions, and would be eligible for DBS. In the USA alone, this corresponds to more than 6000 individuals.[71] However, robust predictors of treatment outcome following DBS have not yet been established, motivating the application of both the lesion and DBS network mapping approaches in the present study. Indeed, combining the two methods (as done here) allowed to predict clinical outcomes following DBS in the treatment of Parkinson's disease and major depression based on lesions causing parkinsonism[38] and depression.[72] Another study focusing on dystonia[39] demonstrated anatomical overlap between a lesion-based network and the network associated with positive outcome after DBS.

In Tourette disorder, a first study has applied DBS network mapping, before,[73] but did not relate DBS network patterns to lesions associated with tics. Furthermore, the study applied normative structural (instead of functional) connectivity and hence results may not be directly comparable to ours. In the study, structural

Table 1 Peak coordinates

Region	Hemisphere	Thalamus R-Map	GPi R-Map	Agreement R-Map	Lesion network map
		X/Y/Z (R-value)	X/Y/Z (R-value)	X/Y/Z (R-value)	X/Y/Z (T-value)
Sub-lobar insula (BA13)	LH	−42/−8/2 (0.66)	−34/−28/14 (0.45)	−34/−28/14 (0.28)	−44/10/−8 (20)
	RH	46/−6/0 (0.67)	42/−18/14 (0.48)	46/−16/10 (0.27)	44/12/−8 (19)
Putamen	LH	−32/−14/−2 (0.68)	−18/6/−6 (0.63)	−30/−6/−8 (0.25)	−20/4/−14 (20)
	RH	34/−18/6 (0.64)	24/4/−10 (0.59)	32/−12/12 (0.20)	20/4/−14 (20)
Cingulate gyrus (limbic lobe)	LH	−6/−6/40 (0.63)	−4/−2/34 (0.64)	0/−10/42 (0.31)	0/12/24 (19)
	RH	4/−14/44 (0.65)	4/−2/34 (0.55)	2/−12/42 (0.27)	10/22/24 (19)
Precentral gyrus	LH	−66/0/10 (0.66)	−68/0/26 (0.46)	−68/0/26 (0.26)	−42/12/2 (19)
	RH	70/4/6 (0.67)	44/18/34 (0.63)	70/6/4 (0.30)	44/8/2 (19)
Mammillary body	LH	−10/−16/−2 (0.77)	−8/−20/−2 (0.08)	−10/−16/−2 (0.06)	−8/−20/−2 (20)
	RH	12/−20/0 (0.57)	12/−22/−2 (0.04)	12/−22/−2 (0.02)	12/−16/−2 (20)
Midbrain	LH	−8/−16/−4 (0.71)	0/−34/0 (0.44)	−6/−30/0 (0.12)	−8/−22/−4 (20)
	RH	16/−22/−4 (0.62)	2/−34/0 (0.53)	16/−26/−4 (0.17)	10/−22/−4 (20)
Medial dorsal nucleus	LH	−10/−18/4 (0.62)	−4/−12/8 (0.58)	−4/−14/6 (0.27)	−6/−20/2 (20)
	RH	14/−20/4 (0.58)	4/−14/10 (0.57)	4/−12/4 (0.25)	8/−20/2 (20)
Ventral posterior medial nucleus	LH	−14/−18/−2 (0.68)	−14/−18/8 (0.17)	−14/−18/8 (0.08)	−16/−22/4 (20)
	RH	18/−20/−2 (0.62)	20/−20/8 (0.26)	18/−20/8 (0.13)	18/−22/6 (20)
Cingulate gyrus (BA24)	LH	−10/−4/40 (0.64)	−2/0/34 (0.65)	−4/−14/40 (0.34)	−2/12/24 (19)
	RH	12/−4/40 (0.64)	4/0/34 (0.59)	4/0/34 (0.27)	8/14/24 (19)
Claustrum	LH	−36/−22/4 (0.65)	−28/6/12 (0.47)	−34/−24/8 (0.21)	−38/−20/−8 (20)
	RH	38/−20/4 (0.65)	34/−14/14 (0.44)	34/−14/14 (0.25)	38/−14/−10 (20)
Pulvinar	LH	−20/−24/2 (0.65)	−6/−28/4 (0.40)	−10/−24/12 (0.17)	−18/−24/4 (20)
	RH	20/−28/2 (0.60)	12/−26/12 (0.30)	20/−22/14 (0.15)	20/−24/6 (20)
Inferior frontal gyrus	LH	−64/12/12 (0.66)	−60/22/26 (0.52)	−64/10/26 (0.22)	−48/14/−10 (19)
	RH	68/10/12 (0.61)	62/30/−4 (0.59)	68/14/24 (0.28)	50/16/−6 (19)
Globus pallidus, pars externa	LH	−26/−16/0 (0.48)	−14/6/−2 (0.48)	−26/−18/0 (0.08)	−20/−4/−10 (19)
	RH	30/−12/−2 (0.50)	22/2/−8 (0.50)	30/−14/−6 (0.14)	18/4/−10 (20)
Globus pallidus, pars interna	LH	−18/−10/0 (0.28)	−12/2/−2 (0.17)	−20/−10/−6 (0)	−16/−8/−10 (0)
	RH	24/−14/−4 (0.32)	16/−2/−6 (0.18)	24/−12/−6 (0.02)	18/−2/−10 (19)

Table summarizes MNI coordinates of regions visualized on different brain connectivity maps presented in the study (Figs 3 and 7). LH = left hemisphere; RH = right hemisphere.

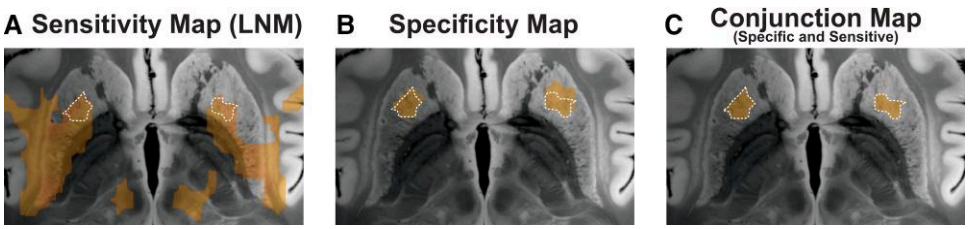

Figure 4 Regions connected to tic-inducing lesions: sensitivity and specificity analysis. Lesion network map (LNM; **A**) represents voxels that were connected to tic-inducing lesions. Specificity of connectivity to lesions associated with occurrence of tics was calculated by contrasting connectivity profiles of lesions associated with tics to a total of 717 lesions from the Harvard Lesion Repository (**B**). This analysis highlighted a region within the anterior striatum that would be specifically linked to tic-occurrence. Voxels that were both specific and sensitive to tic occurrence are demonstrated in **C**. This conjunction map contained voxels that were shown in both **A** and **B**.

connectivity to an extensive array of brain areas was associated with DBS-related modulation of tic severity, including limbic, associative, and sensorimotor networks. Interestingly, structural connectivity patterns were largely inverse between the pallidal and thalamic stimulation targets. Although a strong connectivity to limbic and associative networks, including the cingulate cortex, caudate and thalamus, predicted post-DBS tic improvement in patients who received GPi stimulation ($n = 34$), this was not the case for the thalamic stimulation cohort. In the latter group ($n = 32$), connectivity to primary sensorimotor and parietal-temporal-occipital networks, as well as the putamen, correlated with reduction in tic severity. In part, this matches with our results which showed different optimal connectivity profiles for both pallidal and thalamic target sites—however, here, networks were not inverse to each other, and their common denominator set of regions precisely matched the network identified by lesions. Crucially, structural connectivity analyses as carried out in the aforementioned study[73] cannot detect indirect (i.e. polysynaptic) connections. In our sample, functional connectivity of both pallidal and thalamic cohorts to the same tic-related lesion network was associated with greater tic improvement. Moreover, while in a data-driven analysis of DBS sites, the two optimal connectivity profiles between pallidal and thalamic targets differed, their agreement mapped exactly to the network identified by the lesion analysis. First, these results validate the significance of the tic lesion network in the pathophysiology of tic generation. Second, they provide a functional network template that could inform effective neuromodulatory interventions aimed at reducing tics.

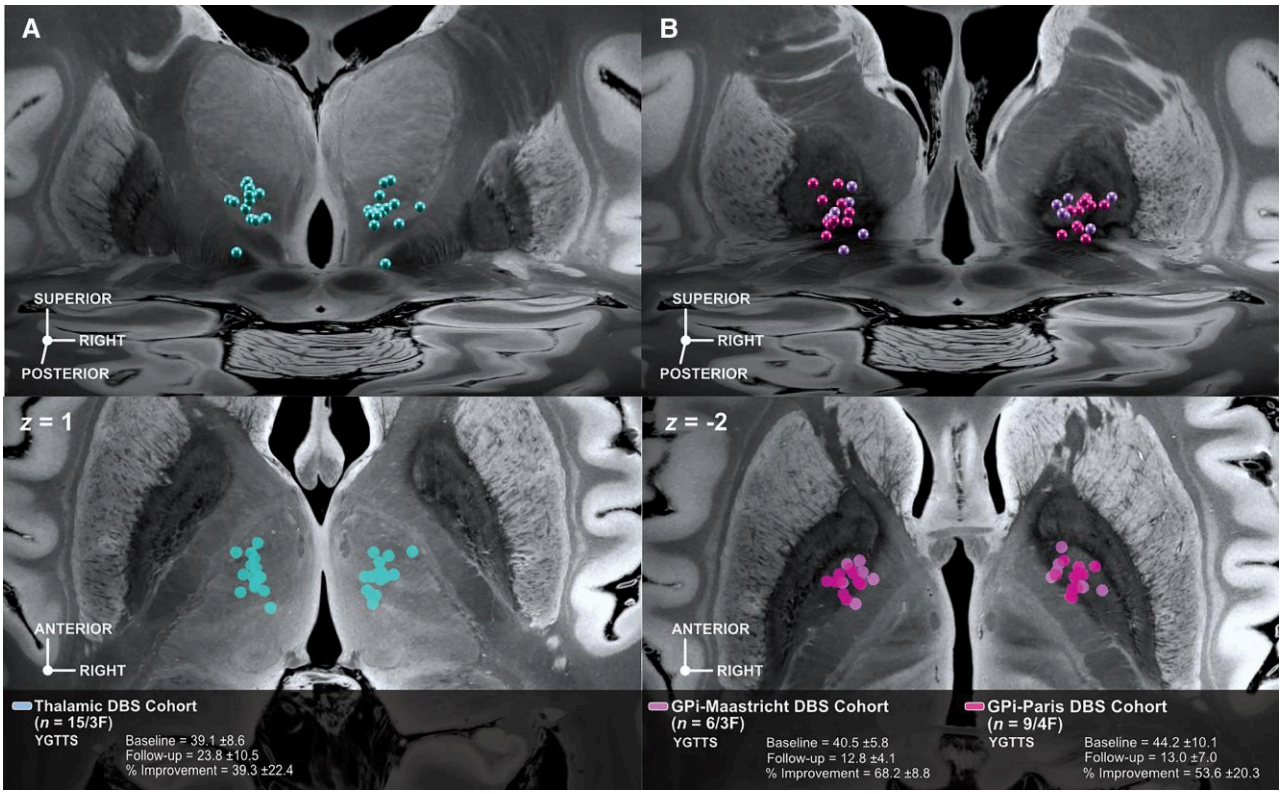

Figure 5 DBS cohorts electrode placement. Each DBS cohort comprises bilaterally implanted electrodes targeting different subcortical regions. The thalamic DBS cohort (**A**) consisted of $n = 15$ patients from the Cologne clinical centre while the GPi cohort (**B**) consisted of six patients from the Maastricht and nine from the Paris clinical centres. Panels show active contact locations relative to anatomical planes defined by the 100 µm post-mortem ultra-high resolution post-mortem template in an oblique 3D view from posterodorsal (*top*) and axial slice (*bottom*) view (where contact sites were orthogonally projected onto the plane).[58]

Limitations

Some noteworthy limitations apply to this study. First, both literature-derived network maps and DBS cases were acquired retrospectively. In the former, causality between brain lesions and occurrence of tics cannot be established with absolute certainty. This has been a longstanding limitation of studying case reports across symptoms and constitutes a true limitation. However, lesions resulting in the emergence of tics are rare and from 22 identified cases, 19 mapped to a shared network. We manually segmented lesion locations on the MNI template, resulting in 2D regions. Prior analyses showed that this would lead to similar connectivity profiles as corresponding 3D lesions[36,74] and the same procedure has been carried out in several lesion network mapping studies that showed robust findings.[38,41–72] Prospective validation of network maps to explain variance in clinical outcome will be crucial to move forward.

Second, we carried out network mapping for both lesions and DBS cases using normative functional connectivity acquired in healthy individuals. This has been done successfully in previous studies yielding results that were used to cross-predict clinical improvement in independent cohorts in a variety of diseases.[42,43,44,45,46–59] At the same time, this approach applies a 'broad lens' view on human brain function and may not reveal patient- or disease-specific details of brain connectivity. The method determines the networks underlying DBS sites or lesions within the average healthy human brain. This notion is crucial when interpreting results but indeed has multiple practical advantages: for instance, lesions (with ischemic tissue) would not show patient-specific network connectivity, even if patient-specific functional scans were available (since the lesion site is not active after stroke). In other words, functional connectivity from stroke sites is not present and cannot be calculated using patient-specific functional MRI data. In both stroke and DBS, distributed brain networks would be altered by the incidents (infarction or neurostimulation) themselves. Here, we ask which networks of the pre-stroke/pre-DBS brain would be affected by both incidents and argue that this would identify exactly the networks with therapeutic value.

Third, the process of DBS electrode reconstruction is prone to inaccuracies that can be relevant, as previously discussed.[53] Moreover, the model applied to estimate stimulation volumes surrounding DBS electrodes applied here may be over-simplistic compared to more elaborate methods.[75,76,77] However, in the context of functional MRI mapping (with an isotropic resolution of 2 mm), subtle inaccuracies of the applied model may not be as impactful as in more fine-grained analyses.

Finally, we note that while both lesions and DBS sites identified a shared network with high spatial overlap, lesions that fell into the network induced tics while DBS to the network alleviated tics. With the methods at hand, we may currently only speculate why that is the case. For one, we believe that the disruption of the network is involved in producing tics and such a disruption could be induced by lesions that corrupt the functionality of the network. How exactly this 'disruption' is mechanistically implemented cannot be investigated with the methods of the present study, but local field potential recordings from both thalamic and pallidal DBS

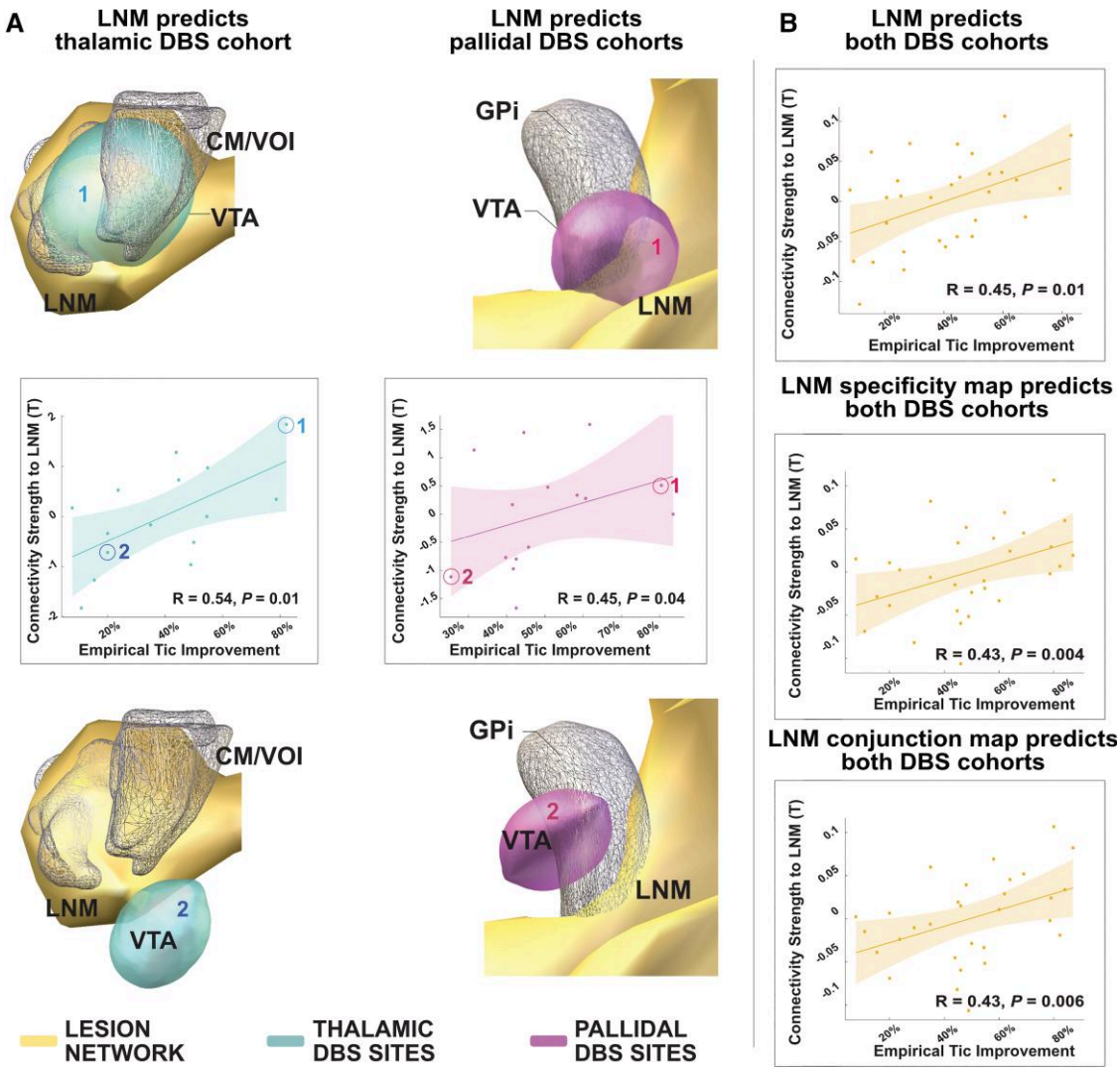

Figure 6 DBS associated tic improvement associates with connectivity to the lesion network map. (**A**) Postoperative percentage improvement of primary tic syndrome from three clinical centres (Cologne-thalamic DBS cohort/turquoise and Paris and Maastricht-pallidal DBS cohort/magenta) associated with the degree of connectivity between either the thalamic or pallidal DBS stimulation sites and the lesion network map. Four example cases of optimal and poor improvements are shown, each demonstrating either strong or weak functional connectivity between the DBS site and the lesion network map, respectively. The lesion network map is shown in yellow, and thalamic stimulation sites in cyan, pallidal ones in purple. Respective example cases are marked in scatter plots. (**B**) Correlation plots between the degree of connectivity of the entire patient cohort and the lesion network map (*top*), the sensitivity map (*middle*), and the conjunction map (*bottom*), respectively. CM/VOI = centromedian nucleus/ventro-oralis nucleus of thalamus; GPi = globus pallidus internus; LNM = lesion network map.

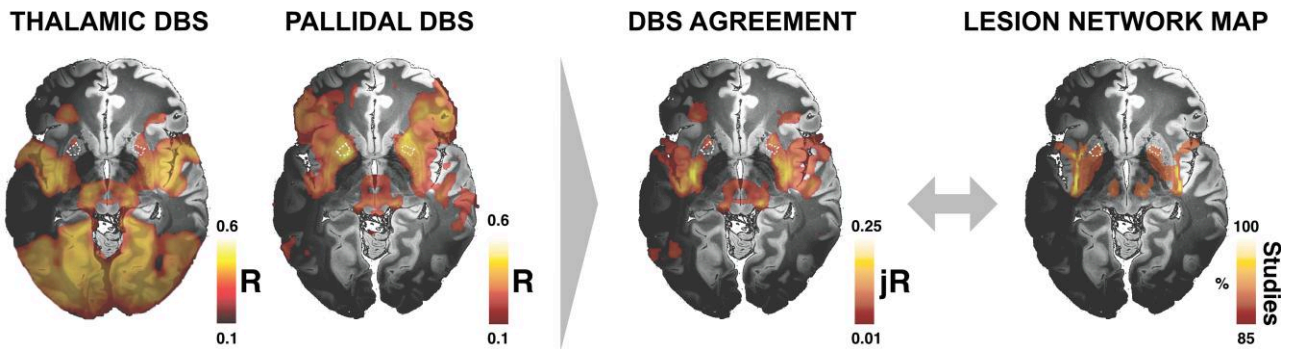

Figure 7 Agreement between DBS and lesion-informed mapping. In a final data-driven analysis, functional connectivity between DBS targets and all other brain areas that correlated with optimal clinical improvement was separately calculated for the thalamic and pallidal cohorts. This led to different connectivity profiles but also included overlapping regions. These are shown as dashed lines in the two maps and by the agreement map. In the agreement map, only regions with positive association in both targets were retained.

electrodes showed that prolonged theta bursts in both targets were associated with preoperative motor tic severity.[16] In other diseases such as Parkinson's disease and dystonia, DBS is known to tone down such aberrant elevated network activity.[78] Hence, our current working model constitutes that lesions (or other aetiologies) could lead to network dysfunction (including the occurrence of noisy feedback carrier signals[79,80]) and DBS could in turn selectively tone down/compensate these aberrant signals, freeing up bandwidth for physiological communication within the network.

Conclusions

This study could associate a functional network including striatal, thalamic, and insular regions of the human brain with (i) the occurrence of tics resulting from brain lesions; and (ii) successful tic reduction following DBS treatment. We could demonstrate that the connectivity between DBS electrodes implanted in two different target sites and our network identified by tic-inducing lesions was able to predict significant amounts of variance in tic improvements. In a data-driven approach, the regions associated with improvement following both pallidal and thalamic DBS mapped to the exact same set of regions identified by the lesion network analysis.

Funding

C.G. is supported by a Freigeist Fellowship of the VolkswagenStiftung. He has received honoraria for educational activities from the Movement Disorder Society. He has served as ad hoc advisory board to Biomarin Pharmaceutical and Lundbeck. J.C.B. and V.V.V. are funded by the Deutsche Forschungsgemeinschaft (DFG, German Research Foundation)—Project-ID 431549029—SFB 1451. M.D.F. was supported by the Nancy Lurie Marks Foundation, the Kaye Family Research Endowment, the Ellison/Baszucki Foundation and the NIH (R01MH113929, R21MH126271, R56AG069086, R01MH115949, and R01AG060987). A.H. was supported by the German Research Foundation (Deutsche Forschungsgemeinschaft, Emmy Noether Stipend 410169619 and 424778381—TRR 295) as well as Deutsches Zentrum für Luft- und Raumfahrt (DynaSti grant within the EU Joint Programme Neurodegenerative Disease Research, JPND). A.H. is participant in the BIH-Charité Clinician Scientist Program funded by the Charité –Universitätsmedizin Berlin and the Berlin Institute of Health. B.A.F., J.F.F., C.H., C.N., D.M., J.L., T.B., L.A., N.P. and Y.W. report no relevant funding for this work.

Competing interests

A.K.K. is a consultant to Boston Scientific and has received honoraria for speaking from Medtronic, Boston Scientific and Abbott, as well as grantsfrom Medtronic, all outside the submitted work. A.F.L. receives royalties from 'Springer Media' and 'De Tijdstroom' Publishers. A.H. reports lecture fees by Boston Scientific unrelated to the present work. The other authors report no competing interests.

Supplementary material

Supplementary material is available at *Brain* online.

References

1. Kurvits L, Martino D, Ganos C. Clinical features that evoke the concept of disinhibition in Tourette syndrome. *Front Psychiatry*. 2020;11:21.
2. Ganos C, Roessner V, Munchau A. The functional anatomy of Gilles de la Tourette syndrome. *Neurosci Biobehav Rev*. 2013;37:1050–1062.
3. Hashemiyoon R, Kuhn J, Visser-Vandewalle V. Putting the pieces together in Gilles de la Tourette syndrome: exploring the link between clinical observations and the biological basis of dysfunction. *Brain Topogr*. 2017;30:3–29.
4. Mink JW. Basal ganglia dysfunction in Tourette's syndrome: a new hypothesis. *Pediatr Neurol*. 2001;25:190–198.
5. Kalanithi PSA, Zheng W, Kataoka Y, *et al*. Altered parvalbumin-positive neuron distribution in basal ganglia of individuals with Tourette syndrome. *Proc Natl Acad Sci U S A*. 2005;102:13307–13312.
6. Kataoka Y, Kalanithi PSA, Grantz H, *et al*. Decreased number of parvalbumin and cholinergic interneurons in the striatum of individuals with Tourette syndrome. *J Comp Neurol*. 2010;518:277–291.
7. Hassler R, Dieckmann G. [Stereotaxic treatment of tics and inarticulate cries or coprolalia considered as motor obsessional phenomena in Gilles de la Tourette's disease]. *Rev Neurol (Paris)*. 1970;123:89–100.
8. Vandewalle V, van der Linden C, Groenewegen HJ, Caemaert J. Stereotactic treatment of Gilles de la Tourette syndrome by high frequency stimulation of thalamus. *The Lancet*. 1999;353:724.
9. Ackermans L, Duits A, van der Linden C, *et al*. Double-blind clinical trial of thalamic stimulation in patients with Tourette syndrome. *Brain*. 2011;134(Pt 3):832–844.
10. Baldermann JC, Kuhn J, Schuller T, *et al*. Thalamic deep brain stimulation for Tourette Syndrome: A naturalistic trial with brief randomized, double-blinded sham-controlled periods. *Brain Stimul*. 2021;14:1059–1067.
11. Baldermann JC, Hennen C, Schüller T, *et al*. A functional network target for tic reduction during thalamic stimulation for Tourette Syndrome. bioRxiv, 2021.
12. Huys D, Bartsch C, Koester P, *et al*. Motor improvement and emotional stabilization in patients with Tourette syndrome after deep brain stimulation of the ventral anterior and ventrolateral motor part of the thalamus. *Biol Psychiatry*. 2016;79:392–401.
13. Kefalopoulou Z, Zrinzo L, Jahanshahi M, *et al*. Bilateral globus pallidus stimulation for severe Tourette's syndrome: a double-blind, randomised crossover trial. *Lancet Neurol*. 2015;14:595–605.
14. Welter ML, Houeto JL, Thobois S, *et al*. Anterior pallidal deep brain stimulation for Tourette's syndrome: a randomised, double-blind, controlled trial. *Lancet Neurol*. 2017;16:610–619.
15. Martinez-Ramirez D, Jimenez-Shahed J, Leckman JF, *et al*. Efficacy and safety of deep brain stimulation in tourette syndrome: The international Tourette syndrome deep brain stimulation public database and registry. *JAMA Neurol*. 2018;75:353–359.
16. Neumann WJ, Huebl J, Brucke C, *et al*. Pallidal and thalamic neural oscillatory patterns in tourette's syndrome. *Ann Neurol*. 2018;84:505–514.
17. Cagle JN, Okun MS, Opri E, *et al*. Differentiating tic electrophysiology from voluntary movement in the human thalamocortical circuit. *J Neurol Neurosurg Psychiatry*. 2020;91:533–539.
18. Priori A, Giannicola G, Rosa M, *et al*. Deep brain electrophysiological recordings provide clues to the pathophysiology of Tourette syndrome. *Neurosci Biobehav Rev*. 2013;37:1063–1068.

19. Karp BI, Porter S, Toro C, Hallett M. Simple motor tics may be preceded by a premotor potential. *J Neurol Neurosurg Psychiatry*. 1996;61:103–106.
20. van der Salm SM, Tijssen MA, Koelman JH, van Rootselaar AF. The bereitschaftspotential in jerky movement disorders. *J Neurol Neurosurg Psychiatry*. 2012;83:1162–1167.
21. Orth M, Munchau A, Rothwell JC. Corticospinal system excitability at rest is associated with tic severity in tourette syndrome. *Biol Psychiatry*. 2008;64:248–251.
22. Franzkowiak S, Pollok B, Biermann-Ruben K, *et al*. Motor-cortical interaction in Gilles de la Tourette syndrome. *PLoS One*. 2012;7:e27850.
23. Martino D, Ganos C, Worbe Y. Neuroimaging applications in Tourette's syndrome. *Int Rev Neurobiol*. 2018;143:65–108.
24. Worbe Y, Gerardin E, Hartmann A, *et al*. Distinct structural changes underpin clinical phenotypes in patients with Gilles de la Tourette syndrome. *Brain*. 2010;133(Pt 12):3649–3660.
25. Draganski B, Martino D, Cavanna AE, *et al*. Multispectral brain morphometry in Tourette syndrome persisting into adulthood. *Brain*. 2010;133(Pt 12):3661–3675.
26. Liu Y, Miao W, Wang J, *et al*. Structural abnormalities in early Tourette syndrome children: a combined voxel-based morphometry and tract-based spatial statistics study. *PLoS One*. 2013;8:e76105.
27. Draper A, Jackson GM, Morgan PS, Jackson SR. Premonitory urges are associated with decreased grey matter thickness within the insula and sensorimotor cortex in young people with Tourette syndrome. *J Neuropsychol*. 2016;10:143–153.
28. Thomalla G, Siebner HR, Jonas M, *et al*. Structural changes in the somatosensory system correlate with tic severity in Gilles de la Tourette syndrome. *Brain*. 2009;132(Pt 3):765–777.
29. Fahim C, Yoon U, Das S, *et al*. Somatosensory–motor bodily representation cortical thinning in Tourette: effects of tic severity, age and gender. *Cortex*. 2010;46:750–760.
30. Sowell ER, Kan E, Yoshii J, *et al*. Thinning of sensorimotor cortices in children with Tourette syndrome. *Nat Neurosci*. 2008;11:637–639.
31. Bohlhalter S, Goldfine A, Matteson S, *et al*. Neural correlates of tic generation in Tourette syndrome: an event-related functional MRI study. *Brain*. 2006;129(Pt 8):2029–2037.
32. Neuner I, Werner CJ, Arrubla J, *et al*. Imaging the where and when of tic generation and resting state networks in adult Tourette patients. *Front Hum Neurosci*. 2014;8:362.
33. Tinaz S, Malone P, Hallett M, Horovitz SG. Role of the right dorsal anterior insula in the urge to tic in Tourette syndrome. *Mov Disord*. 2015;30:1190–1197.
34. Worbe Y, Sgambato-Faure V, Epinat J, *et al*. Towards a primate model of Gilles de la Tourette syndrome: anatomo-behavioural correlation of disorders induced by striatal dysfunction. *Cortex*. 2013;49:1126–1140.
35. Fox MD. Mapping symptoms to brain networks with the human connectome. *N Engl J Med*. 2018;379:2237–2245.
36. Boes AD, Prasad S, Liu H, *et al*. Network localization of neurological symptoms from focal brain lesions. *Brain*. 2015;138(Pt 10):3061–3075.
37. Laganiere S, Boes AD, Fox MD. Network localization of hemichorea-hemiballismus. *Neurology*. 2016;86:2187–2195.
38. Joutsa J, Horn A, Hsu J, Fox MD. Localizing parkinsonism based on focal brain lesions. *Brain*. 2018;141:2445–2456.
39. Corp DT, Joutsa J, Darby RR, *et al*. Network localization of cervical dystonia based on causal brain lesions. *Brain*. 2019;142:1660–1674.
40. Darby RR, Joutsa J, Burke MJ, Fox MD. Lesion network localization of free will. *Proc Natl Acad Sci U S A*. 2018;115:10792–10797.
41. Darby RR, Horn A, Cushman F, Fox MD. Lesion network localization of criminal behavior. *Proc Natl Acad Sci U S A*. 2018;115:601–606.
42. Horn A, Reich M, Vorwerk J, *et al*. Connectivity predicts deep brain stimulation outcome in Parkinson disease. *Ann Neurol*. 2017;82:67–78.
43. Irmen F, Horn A, Mosley P, *et al*. Left prefrontal connectivity links subthalamic stimulation with depressive symptoms. *Ann Neurol*. 2020;87:962–975.
44. Al-Fatly B, Ewert S, Kubler D, Kroneberg D, Horn A, Kuhn AA. Connectivity profile of thalamic deep brain stimulation to effectively treat essential tremor. *Brain*. 2019;142:3086–3098.
45. Baldermann JC, Melzer C, Zapf A, *et al*. Connectivity profile predictive of effective deep brain stimulation in obsessive-compulsive disorder. *Biol Psychiatry*. 2019;85:735–743.
46. Li N, Baldermann JC, Kibleur A, *et al*. A unified connectomic target for deep brain stimulation in obsessive-compulsive disorder. *Nat Commun*. 2020;11:3364.
47. Siddiqi SH, Schaper FLWVJ, Horn A, *et al*. Brain stimulation and brain lesions converge on common causal circuits in neuropsychiatric disease. *Nat Hum Behav*. 2021;5(12):1707–1716.
48. Horn A, Kuhn AA. Lead-DBS: a toolbox for deep brain stimulation electrode localizations and visualizations. *Neuroimage*. 2015;107:127–135.
49. Holmes AJ, Hollinshead MO, O'Keefe TM, *et al*. Brain Genomics Superstruct Project initial data release with structural, functional, and behavioral measures. *Sci Data*. 2015;2:150031.
50. Yeo BT, Krienen FM, Sepulcre J, *et al*. The organization of the human cerebral cortex estimated by intrinsic functional connectivity. *J Neurophysiol*. 2011;106:1125–1165.
51. Cohen AL, Fox MD. Reply: the influence of sample size and arbitrary statistical thresholds in lesion-network mapping. *Brain*. 2020;143:e41.
52. Eklund A, Nichols TE, Knutsson H. Cluster failure: why fMRI inferences for spatial extent have inflated false-positive rates. *Proc Natl Acad Sci U S A*. 2016;113:7900–7905.
53. Horn A, Li N, Dembek TA, *et al*. Lead-DBS v2: towards a comprehensive pipeline for deep brain stimulation imaging. *Neuroimage*. 2019;184:293–316.
54. Avants BB, Epstein CL, Grossman M, Gee JC. Symmetric diffeomorphic image registration with cross-correlation: evaluating automated labeling of elderly and neurodegenerative brain. *Med Image Anal*. 2008;12:26–41.
55. Husch A, Petersen MV, Gemmar P, Goncalves J, Hertel F. PaCER - a fully automated method for electrode trajectory and contact reconstruction in deep brain stimulation. *Neuroimage Clin*. 2018;17:80–89.
56. van Albada SJ, Robinson PA. Transformation of arbitrary distributions to the normal distribution with application to EEG test-retest reliability. *J Neurosci Methods*. 2007;161:205–211.
57. Li N, Hollunder B, Baldermann JC, *et al*. A unified functional network target for deep brain stimulation in obsessive-compulsive disorder. *Biol Psychiatry* 2021;90:701–713.
58. Edlow BL, Mareyam A, Horn A, *et al*. 7 Tesla MRI of the ex vivo human brain at 100 micron resolution. *Sci Data*. 2019;6:244.
59. Horn A, Fox MD. Opportunities of connectomic neuromodulation. *Neuroimage*. 2020;221:117180.
60. Lozano AM, Lipsman N. Probing and regulating dysfunctional circuits using deep brain stimulation. *Neuron*. 2013;77:406–424.
61. McCairn KW, Nagai Y, Hori Y, *et al*. A primary role for nucleus accumbens and related limbic network in vocal tics. *Neuron*. 2016;89:300–307.
62. Balthasar K. [The anatomical substratum of the generalized tic disease (maladie des tics, Gilles de la Tourette); arrest of

development of the corpus striatum]. *Arch Psychiatr Nervenkr Z Gesamte Neurol Psychiatr*. 1957;195:531–549.
63. Johnson KA, Fletcher PT, Servello D, *et al*. Image-based analysis and long-term clinical outcomes of deep brain stimulation for Tourette syndrome: a multisite study. *J Neurol Neurosurg Psychiatry*. 2019;90:1078–1090.
64. Swanson LW. Cerebral hemisphere regulation of motivated behavior. *Brain Res*. 2000;886:113–164.
65. Chia Z, Augustine GJ, Silberberg G. Synaptic connectivity between the cortex and claustrum is organized into functional modules. *Curr Biol*. 2020;30:2777–2790.e4.
66. Choi EY, Yeo BTT, Buckner RL. The organization of the human striatum estimated by intrinsic functional connectivity. *J Neurophysiol*. 2012;108:2242–2263.
67. McCutcheon RA, Abi-Dargham A, Schizophrenia HO. Schizophrenia, dopamine and the striatum: from biology to symptoms. *Trends Neurosci*. 2019;42:205–220.
68. Nieuwenhuys R, Voogd J, van Huijzen C. *The human central nervous system*. 4th ed. Springer; 2008:xiv, 967 p.
69. McCairn KW, Iriki A, Isoda M. Global dysrhythmia of cerebro-basal ganglia-cerebellar networks underlies motor tics following striatal disinhibition. *J Neurosci*. 2013;33:697–708.
70. Tremblay L, Worbe Y, Thobois S, Sgambato-Faure V, Feger J. Selective dysfunction of basal ganglia subterritories: from movement to behavioral disorders. *Mov Disord*. 2015;30:1155–1170.
71. Martino D, Deeb W, Jimenez-Shahed J, *et al*. The 5 pillars in Tourette syndrome deep brain stimulation patient selection: present and future. *Neurology*. 2021;96:664–676.
72. Padmanabhan JL, Cooke D, Joutsa J, *et al*. A human depression circuit derived from focal brain lesions. *Biol Psychiatry*. 2019;86:749–758.
73. Johnson KA, Duffley G, Anderson DN, *et al*. Structural connectivity predicts clinical outcomes of deep brain stimulation for Tourette syndrome. *Brain*. 2020;143:2607–2623.
74. Darby RR, Laganiere S, Pascual-Leone A, Prasad S, Fox MD. Finding the imposter: brain connectivity of lesions causing delusional misidentifications. *Brain*. 2017;140:497–507.
75. Gunalan K, Chaturvedi A, Howell B, *et al*. Creating and parameterizing patient-specific deep brain stimulation pathway-activation models using the hyperdirect pathway as an example. *PLoS One*. 2017;12:e0176132.
76. Duffley G, Anderson DN, Vorwerk J, Dorval AD, Butson CR. Evaluation of methodologies for computing the deep brain stimulation volume of tissue activated. *J Neural Eng*. 2019;16:066024.
77. Howell B, Gunalan K, McIntyre CC. A driving-force predictor for estimating pathway activation in patient-specific models of deep brain stimulation. *Neuromodulation*. 2019;22:403–415.
78. Kuhn AA, Volkmann J. Innovations in deep brain stimulation methodology. *Mov Disord*. 2017;32:11–19.
79. Horn A, Al-Fatly B, Neumann WJ, Neudorfer C. Chapter 1 - Connectomic DBS: an introduction. In: Horn A, ed. *Connectomic Deep Brain Stimulation*. Academic Press; 2022:3–23.
80. Brown P. Oscillatory nature of human basal ganglia activity: relationship to the pathophysiology of Parkinson's disease. *Mov Disord*. 2003;18(4):357–363.